SOM-LS: Selective Orthogonal Matrix Least-Squares Method for Macromodeling Multiport Networks Characterized by Sampled Data

Yuichi Tanji, Takayuki Watanabe**, and Hideki Asai****

*Dept. of RISE, Kagawa University, Japan

**School of Administration & Informatics, University of Shizuoka, Japan

***Dept. of Systems Eng., Shizuoka University, Japan

Abstract

This paper presents the selective orthogonal matrix least-squares (SOM-LS) method for representing a multiport network characterized by sampled data with the rational matrix. Recently, it is needed in a circuit design to evaluate physical effects of interconnects and package, and the evaluation is done by numerical electromagnetic analysis or measurement by network analyzer. Here, the SOM-LS method will play an important role for generating the macromodels of interconnects and package in circuit simulation level. The accuracy of the macromodels is predictable and controllable, that is, the SOM-LS method fits the rational matrix to the sampled data, selecting the dominant poles of the rational matrix. In examples, simple PCB models are analyzed, where the rational matrices are described by Verilog-A, and some simulations are carried out on a commercial circuit simulator.

1. Introduction

Designers of mixed analog/digital circuits begin to employ top-down design and bottom-up verification methodologies [1], [2]. Due to the continued consumerization of the electronics market place, electronics companies are required to develop these products very rapidly in order to ensure the market share. Therefore, utilizing higher levels of abstraction, the designers intend to cope with complexities in the designs and shorten the developing periods. On the other hand, physical effects such as interconnects and power consumption to be observed at lower levels have been increasingly significant in the overall performance of the systems [3]. Furthermore, owing to success of shrinking process technologies, the micromechanical systems are to be implemented as system-on-chip [4]. In these cases, low level effects must be involved in models at higher levels of abstraction.

Model reduction algorithms [6]-[15] are suitable for producing the higher level models. These methods provide a small system from a set of equations fully described by the lower levels of details. The moment matching techniques [6], [7] and PVL [8] provide a lower order rational function for linear time-invariant single-input single-output (SISO) system. Furthermore, Krylov subspace methods [9]-[11] obtain the reduced-order models of linear time-invariant multi-input multi-output (MIMO) systems projecting them into subspaces of lower dimensions. These ideas have been also applied to model reduction of linear time-varying systems [13] and weakly [14] or general nonlinear ones [15], focusing on applications to communication [13], [14] and micromachine [15]. These model reduction algorithms generate the models without requiring additional modeling expertises from designers, and the accuracy of the models are relatively predictable and controllable using Krylov projection methods with error bound [12].

Besides the availability of model reduction algorithms, numerical methods for electromagnetic analysis such as finite elements (FEM) method [16], the method of moment (MoM) [17], and finite difference time domain (FDTD) method [18], and measurement by network analyzer are widely employed in the fields of package and microwave. Since the system level behaviors then are given by sampled data in the time or frequency-domain with multiport networks expressed by admittance, impedance, and scattering matrices, many researchers have paid their attentions to approximation of the sampled data by a rational matrix [19]-[27]. The essence of the rational approximation is to fit the rational matrix to the sampled data by the least-squares (LS) methods. The LS fitting based macromodeling methods, however, could not preserve the passivity of the original systems, which was fault of these methods in comparing to the model reduction algorithms for linear time-invariant systems [10], [11]. Fortunately, enforcing the rational matrix to be passive has been reported in the recent published works [26], [27].

In this paper, we present a method for approximating sampled data by the rational matrix. First, the sampled data, which are frequency-domain data of network parameter matrix, are separately approximated by a rational function, then, we can obtain the poles from the rational functions. Next, the residues are determined by the orthogonal LS method so that the rational matrix consisting of the poles and residues is fitted to the sampled data for all the elements of the network parameter matrix. Here, the accuracy of the rational matrix is predictable and controllable, that is, the LS method fits the rational matrix to the sampled data, selecting the dominant poles. Selection of the dominant poles is corresponding to choosing the orthogonal vectors in orthogonalization steps for solving the matrix equation with respect to the residues. We call this method the selective orthogonal matrix least-squares (SOM-LS) method.

It is known that the LS methods minimize 2-norm of the residual matrix which is defined as the difference between the right- and left-hand sides of the matrix equation [33]. Here, it is considered that the algorithms reach the minimum points via the process that the 2-norm of residual matrix decreases monotonously during the orthogonalization steps. Therefore, the 2-norm gives error bound of the LS methods. The SOM-LS method exploits the feature of 2-norm and provides the least-squares solution. This method is based on the Chen's method [31] for SISO nonlinear system identification. In the Chen's method, coupling coefficients of nonlinear functions are determined using the LS method for SISO systems so that the linear constraints are satisfied. The SOM-LS method is the extension of the Chen's LS method to MIMO systems. Although the objective of this paper is to model linear time-invariant multiport networks characterized by sampled data, this procedure will be also applicable to nonlinear systems by using nonlinear functions such as radial basis function (RBF) [30] that composes a neural network.

This paper is organized as follows. The section II presents the SOM-LS method for approximating sampled data by the rational matrix. The section III presents how to describe the rational matrix in the format of Verilog-A which is language for describing analog parts of mixed analog/digital circuits on Verilog-AMS [1]. The simulation results are obtained by a commercial circuit simulator, and the proposed procedure will be demonstrated to be effective. Some conclusions are given in the final section.

2. Selective Orthogonal Matrix Least Squares Method

In this section, a powerful method, so-called the selective orthogonal matrix least-squares (SOM-LS) method, for representing multiport networks characterized by sampled data with the rational matrix, is presented.

2.1. Determining Poles

The goal of this section is to approximate sampled data by the rational matrix:

$$\boldsymbol{Y}(s) \quad = \quad \boldsymbol{K}_0 + \sum_{i=1}^{N} \frac{1}{s - p_i} \boldsymbol{K}_i, \tag{1}$$

where $\boldsymbol{K}_i$, p_i, and $\boldsymbol{Y}(s)$ are residue matrix, pole, and parameter matrix, respectively. Since the poles p_i $(i = 1, 2, \ldots, N)$ are unknown, we have to extract them from the sampled data. Therefore, each element of the parameter matrix is separately approximated by the rational function using the weighted LS method [21]. At many points ω_l $(l = 0, 1, \ldots, M)$ on the imaginary axis in the complex plane, each element is enforced as

$$y_{ij}(j\omega_l) \quad = \quad \frac{b_0 + b_1 j\omega_l + b_2 (j\omega_l)^2 + \cdots + b_n (j\omega_l) s^n}{1 + a_1 (j\omega_l) + a_2 (j\omega_l)^2 + \cdots + a_n (j\omega_l)^n}. \tag{2}$$

When the frequency points ω_l are in a wide range, the weighted LS method for constructing (2) sometimes becomes ill-conditioned. Therefore, the frequency range should be partitioned into some regions, and the sampled data are approximated in each region [24].

2.2. Matrix Rational Approximation

Using N poles obtained by the weighted LS method, the sampled data are represented by the rational matrix. Then, the rational matrix is constrained as

$$\boldsymbol{Y}(j\omega_l) \quad = \quad \boldsymbol{K}_0 + \sum_{i=1}^{N} \frac{1}{j\omega_l - p_i} \boldsymbol{K}_i. \tag{3}$$
$$(l \quad = \quad 0, 1, \ldots, M)$$

However, one must desire a more compact model for efficient simulation. To achieve it, we need to select the dominant poles from p_i $(i = 1, \ldots, N)$. The next subsection provides a property of the orthogonal matrix least-squares (OM-LS) method which is employed to select the dominant poles and approximate the sampled data with the SOM-LS method.

2.3. Property of OM-LS Method

Equation (3) is enforced in LS sense, then, a matrix equation is solved in order to determine the residue matrices $\boldsymbol{K}_i$ $(i = 1, 2, \ldots, N)$. We assume the matrix equation as

$$\boldsymbol{PH} \quad = \quad \boldsymbol{F}, \tag{4}$$

where $\boldsymbol{P}$ is the coefficient matrix constructed from (3), $\boldsymbol{H}$ is a matrix consisting of the residue matrices, and $\boldsymbol{F}$ is a matrix whose entries are values of the parameter matrix $\boldsymbol{Y}(s)$ of (1) at the points ω_l $(l = 0, 1, \ldots, M)$ [24].

(4) is solved using the QR decomposition:

$$\boldsymbol{P} \quad = \quad \boldsymbol{WA}, \tag{5}$$

where $\boldsymbol{W}$ and $\boldsymbol{A}$ are orthogonal and upper triangle matrices. Then, the solution $\boldsymbol{H}$ can be written by

$$\boldsymbol{G} \quad = \quad \left(\boldsymbol{W}^T \boldsymbol{W}\right)^{-1} \boldsymbol{W}^T \boldsymbol{F} \tag{6}$$
$$\boldsymbol{H} \quad = \quad \boldsymbol{A}^{-1} \boldsymbol{G}. \tag{7}$$

The process of (6) and (7) is called the OM-LS method [31]. The rest part of this subsection presents a property of this method, which is useful for selecting the dominant poles from p_i $(i = 1, 2, \ldots, N)$ obtained from the weighted LS method.

The matrices $\boldsymbol{P}$ and $\boldsymbol{W}$ are rewritten using the column vectors as

$$\boldsymbol{P} \quad = \quad (\boldsymbol{p}_1, \boldsymbol{p}_2, \ldots, \boldsymbol{p}_N) \tag{8}$$
$$\boldsymbol{W} \quad = \quad (\boldsymbol{w}_1, \boldsymbol{w}_2, \ldots, \boldsymbol{w}_N). \tag{9}$$

For $N \geq n$, we define the residual matrix of (4) as

$$\boldsymbol{Z}_n \quad = \quad \boldsymbol{F} - \boldsymbol{W}_n \boldsymbol{G}_n, \tag{10}$$

where

$$\boldsymbol{W}_n \quad = \quad (\boldsymbol{w}_1, \boldsymbol{w}_2, \ldots, \boldsymbol{w}_n)^T$$
$$\boldsymbol{G}_n \quad = \quad (\boldsymbol{g}_1, \boldsymbol{g}_2, \ldots, \boldsymbol{g}_n)^T.$$

The product $\boldsymbol{Z}_n^T \boldsymbol{Z}_n$ satisfies

$$\boldsymbol{Z}_n^T \boldsymbol{Z}_n \quad = \quad \boldsymbol{F}^T \boldsymbol{F} - \sum_{i=1}^{n} \boldsymbol{w}_i^T \boldsymbol{w}_i \boldsymbol{g}_i \boldsymbol{g}_i^T. \tag{11}$$

The 2-norm of the residual matrix holds the following theorem.

Theorem 1 *The sequence* $\{||\boldsymbol{Z}_1||_2, ||\boldsymbol{Z}_2||_2, \ldots, ||\boldsymbol{Z}_n||_2\}$ *decreases monotonously.*

Proof) Equation (11) is rewritten by

$$\boldsymbol{Z}_n^T \boldsymbol{Z}_n \quad = \quad \boldsymbol{Z}_{n-1}^T \boldsymbol{Z}_{n-1} - \boldsymbol{w}_n^T \boldsymbol{w}_n \boldsymbol{g}_n \boldsymbol{g}_n^T. \tag{12}$$

For $\boldsymbol{x} \neq \boldsymbol{0}$, the quadratic form of (12) is written by

$$\boldsymbol{x}^T \boldsymbol{Z}_n^T \boldsymbol{Z}_n \boldsymbol{x} \quad = \quad \boldsymbol{x}^T \boldsymbol{Z}_{n-1}^T \boldsymbol{Z}_{n-1} \boldsymbol{x} - \boldsymbol{w}_n^T \boldsymbol{w}_n \boldsymbol{x}^T \boldsymbol{g}_n \boldsymbol{g}_n^T \boldsymbol{x}. \tag{13}$$

Dividing (13) with $\boldsymbol{x}^T \boldsymbol{x}$, we write the maximum value as

$$\max_{\boldsymbol{x} \neq 0} \frac{\boldsymbol{x}^T \boldsymbol{Z}_n^T \boldsymbol{Z}_n \boldsymbol{x}}{\boldsymbol{x}^T \boldsymbol{x}} \quad = \quad \frac{\tilde{\boldsymbol{x}}^T \boldsymbol{Z}_{n-1}^T \boldsymbol{Z}_{n-1} \tilde{\boldsymbol{x}}}{\tilde{\boldsymbol{x}}^T \tilde{\boldsymbol{x}}} - \boldsymbol{w}_n^T \boldsymbol{w}_n \frac{\tilde{\boldsymbol{x}}^T \boldsymbol{g}_n \boldsymbol{g}_n^T \tilde{\boldsymbol{x}}}{\tilde{\boldsymbol{x}}^T \tilde{\boldsymbol{x}}}. \tag{14}$$

Assuming that

$$\max_{\boldsymbol{x} \neq 0} \frac{\boldsymbol{x}^T \boldsymbol{Z}_{n-1}^T \boldsymbol{Z}_{n-1} \boldsymbol{x}}{\boldsymbol{x}^T \boldsymbol{x}} \quad = \quad \frac{\boldsymbol{x}^{*T} \boldsymbol{Z}_{n-1}^T \boldsymbol{Z}_{n-1} \boldsymbol{x}^*}{\boldsymbol{x}^{*T} \boldsymbol{x}^*}, \tag{15}$$

we have

$$\frac{\boldsymbol{x}^{*T} \boldsymbol{Z}_{n-1}^T \boldsymbol{Z}_{n-1} \boldsymbol{x}^*}{\boldsymbol{x}^{*T} \boldsymbol{x}^*} \quad \geq \quad \frac{\tilde{\boldsymbol{x}}^T \boldsymbol{Z}_{n-1} \boldsymbol{Z}_{n-1}^T \tilde{\boldsymbol{x}}}{\tilde{\boldsymbol{x}}^T \tilde{\boldsymbol{x}}}. \tag{16}$$

As a result, the inequality

$$\max_{\boldsymbol{x} \neq 0} \frac{\boldsymbol{x}^T \boldsymbol{Z}_{n-1}^T \boldsymbol{Z}_{n-1} \boldsymbol{x}}{\boldsymbol{x}^T \boldsymbol{x}} \quad > \quad \max_{\boldsymbol{x} \neq 0} \frac{\boldsymbol{x}^T \boldsymbol{Z}_n^T \boldsymbol{Z}_n \boldsymbol{x}}{\boldsymbol{x}^T \boldsymbol{x}} \tag{17}$$

holds. This means $||\boldsymbol{Z}_{n-1}||_2 > ||\boldsymbol{Z}_n||_2$. □

Note that the 2-norm of $\boldsymbol{Z}_n$ is evaluated by the maximum eigenvalue of $\boldsymbol{Z}_n^T \boldsymbol{Z}_n$, which is used on the implementation of the SOM-LS method.

2.4. SOM-LS Method

LS problems are encountered in various science and engineering aspects. When a system is identified by a network consisting of nonlinear/linear functions, we must determine the coupling coefficients between these functions. The typical example is neural network. Chen *et al.* present a learning algorithm for radial basis function (RBF) networks [30], where the selective orthogonal LS method [31] is used for satisfying the linear constraints. However, all the functions are not necessarily essential. Hence, Chen provided the compact RBF network model by selecting RBF's, where selecting RBF's is corresponding to choosing the orthogonal vectors in orthogonalization steps of the LS method. In this subsection, we present the general version of the Chen's LS method, which is an extention to MIMO systems. Although target of this paper is to approximate the sampled data obtained from a linear time-invariant system, with the rational matrix of complex s, the SOM-LS method will be applicable to MIMO nonlinear system identification. For example, the behavioral modelings using RBF networks [28], [29] can be extended to MIMO systems.

We present the SOM-LS method using the modified Gram-Schmidt (MGS) method. However, the idea can be easily extended to the Householder based algorithm [31] which is more sophisticated than one based on MGS.

The MGS method for solving (4) is summarized below.

MGS()
{
 $\alpha_{k,i}:\ (k,i)$ element of $\boldsymbol{A}$ $(\alpha_{k,k}=1)$

 $\boldsymbol{p}_i^{(0)}=\boldsymbol{p}_i\ \ (i=1,\ldots,N)$
 $\boldsymbol{Z}_0=\boldsymbol{F}$
 for (k = 1; k < N; k++) {
  $\boldsymbol{w}_k=\boldsymbol{p}_k^{(k-1)}$
  $\alpha_{k,i}=\dfrac{\boldsymbol{w}_k^T\boldsymbol{p}_i^{(k-1)}}{\boldsymbol{w}_k^T\boldsymbol{w}_k}$ (i = k+1, ..., N)
  $\boldsymbol{p}_i^{(k)}=\boldsymbol{p}_i^{(k-1)}-\alpha_{k,i}\boldsymbol{w}_k$ (i = k+1, ..., N)
  $\boldsymbol{g}_k^T=\dfrac{\boldsymbol{w}_k^T\boldsymbol{F}^{(k-1)}}{\boldsymbol{w}_k^T\boldsymbol{w}_k}$
  $\boldsymbol{Z}_k=\boldsymbol{Z}_{k-1}-\boldsymbol{w}_k\boldsymbol{g}_k^T$
 }
 $\boldsymbol{w}_N=\boldsymbol{p}_N^{(N-1)}$
}

At the kth iteration of $\mathbf{MGS}()$, the coefficient matrix $\boldsymbol{P}\equiv\boldsymbol{P}^{(k-1)}$ is described by

$$\boldsymbol{P}^{(k-1)} = \left(\boldsymbol{w}_1,\ldots,\boldsymbol{w}_{k-1},\boldsymbol{p}_k^{(k-1)},\ldots,\boldsymbol{p}_N^{(k-1)}\right). \quad (18)$$

By $k-1$ iterations, $k-1$ columns are orthogonalized and $\boldsymbol{w}_1,\ldots,\boldsymbol{w}_{k-1}$ have been obtained. Then we can select one of the vectors $\boldsymbol{p}_k^{(k-1)},\ldots,\boldsymbol{p}_N^{(k-1)}$ as the kth orthogonal vector $\boldsymbol{w}_k$. *Theorem 1* holds regardless of the way how to choose the orthogonal vector, which means that the 2-norm of the residual matrix (10) decreases monotonously during the orthogonalization steps and reaches a fixed value. Therefore, the 2-norm gives error bound of the LS fitting. Hence, we determine $\boldsymbol{w}_k$ so that the 2-norm is greatly reduced at each step. Since each column $\boldsymbol{p}_i^{(k-1)}$ is corresponding to a pole, selection of the dominant poles and approximation of the sampled data is accomplished by the selective orthogonalization procedure.

Fig. 1 shows an example of the SOM-LS method (detail of this example will be given in Sect. 4), where *SOM-LS* is the result obtained by the SOM-LS method and *OM-LS* is the non-selective case. We can see that the 2-norm reaches the fixed value in both cases and *SOM-LS* is more quickly reduced than *OM-LS*. A more compact model would be obtained by terminating the orthogonalization steps.

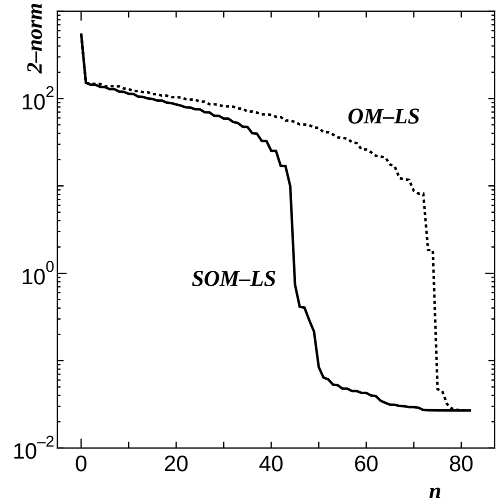

Figure 1: 2-norm of the residual matrix $\boldsymbol{Z}_n$.

2.5. Implementation

Matrix rational approximation of sampled data is implemented as follows. Before applying the SOM-LS method, the following preprocessing is needed.

- The sampled data of parameter matrix (e.g., admittance, impedance, or scattering matrix) of multi-port networks are separately approximated by the rational functions as (2), where upper (or lower) triangular entries of the parameter matrix are only approximated when the matrix is symmetric.
- From the feature of parameter matrix, we can find same poles from different elements [32]. Therefore, the duplicate poles should be eliminated in order to avoid that the matrix $\boldsymbol{P}$ of (4) becomes singular.
- The coefficient matrix $\boldsymbol{P}$ is made from single poles, real and imaginary parts of complex poles [24].

The selective orthogonalization is summarized as Fig. 2, where $\{\mathbf{d},\mathbf{S1},\ldots,\mathbf{R2},\mathbf{I2}\}$ are column vectors of the matrix $\boldsymbol{P}$, and $\mathbf{d}$, $\mathbf{S}$, $\mathbf{R}$, and $\mathbf{I}$ imply direct coupling, single pole, real part of complex pole, and the imaginary part, respectively. First, $\mathbf{S2}$ is orthogonalized (selected) if the residual matrix has the largest 2-norm, and the shift operation is carried out as shown in the second row of Fig. 2. Next, assuming that the residual matrix with $\mathbf{R1}$ has the largest 2-norm, we execute the shift operation and orthogonalization similarly. However, the next step is different from the previous two cases. Since $\mathbf{R1}$ and $\mathbf{I1}$ are related to each other, they must not be separated. Therefore, the shift operation and orthogonalization of $\mathbf{I1}$ is followed by one for $\mathbf{R1}$.

The SOM-LS method is terminated if the condition

$$||\boldsymbol{Z}_n||_2<\delta \quad (19)$$

is satisfied, where δ is a user-defined criterion.

3. Examples

Example 1: Transmission line

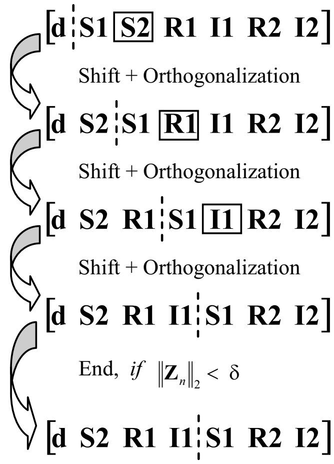

Figure 2: Summary of the SOM-LS method for matrix rational approximation.

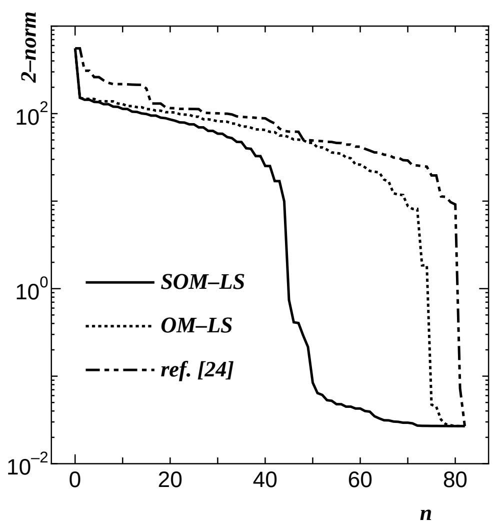

Figure 3: 2-norm in using [25].

The single conductor transmission line (0.5 $[\Omega/$ cm$]$, 10.0 $[nH/$cm$]$, 0.004 $[nF/$cm$]$, 0.0005 $[S/$cm$]$, and the length is 1 [cm]) was used to evaluate the SOM-LS method, where the scattering matrix with 10 $[\Omega]$ reference impedance was approximated. First, the sampled data of upper half elements of the scattering matrix were approximated for every GHz by rational functions, and we obtained 6 single poles and 147 conjugate pairs from 3 elements of the scattering matrix totally. According to the preprocessing, 3 single poles and 39 conjugate pairs were selected. Using the 81 poles, the matrix rational approximation was done. Fig. 2 shows the 2-norm in using the SOM-LS method and the one obtained by the OM-LS method, where *SOM-LS* and *OM-LS* in this figure indicate the results obtained from the SOM-LS and OM-LS methods, respectively. We can see that the reduction ratio of *SOM-LS* is greater than *OM-LS*.

The results were also compared with the previous work [25]. The selective orthogonalization procedure in the previous work is based on the estimator

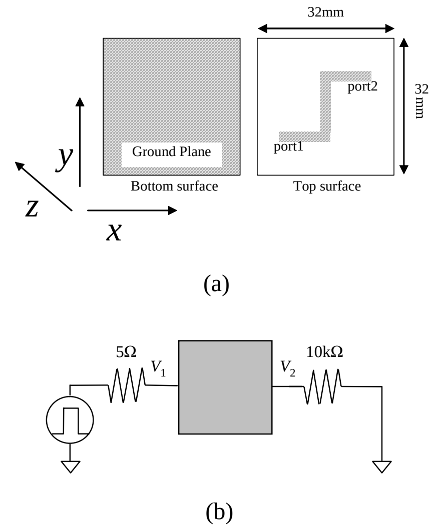

Figure 4: PCB model and circuit of *Example 2*. (a)PCB model. (b)Circuit.

$$\sqrt{\sum_{i=1}^{L}\sum_{j=1}^{L}\left|\frac{g_{i,n}g_{j,n}\boldsymbol{w}_k^T\boldsymbol{w}_k}{\xi_{i,j}}\right|^2},$$

where $\boldsymbol{g}_n = (g_{1,n}\dots g_{L,n}) \in R^L$ and $\xi_{i,j,n}$ is (i,j) element of the matrix $\boldsymbol{F}^T\boldsymbol{F} \in R^{L\times L}$ in (10). This criteria is similar to the Chen's original work for SISO system identification [31], but it is unrelated to the feature of the LS method given by *Theorem 1*. Therefore, this method does not necessarily yield desirable reduction of the 2-norm as shown in Fig. 3. From this fact, we can say that using of 2-norm of the residual matrix at each orthogonalization step is suitable for the SOM-LS method.

Example 2: Interconnect with linear termination on PCB

The simple PCB model shown in Fig. 4(a) was analyzed by the FDTD method, where the cell size was 0.8 $[mm]$ in both of x and y directions and 0.1 $[mm]$ in z direction. Then, the sampled data obtained from the FDTD method were represented by the rational matrix using the SOM-LS method. The SOM-LS method selected 8 poles from 204 poles. Fig. 5 shows the approximation results of admittance matrix of the PCB model.

The rational matrix was described by Verilog-A, and the transient analysis of the circuit shown in 4(b) was carried out on *Cadence Spectre* [35]. Although the time-domain response is obtained by an explicit numerical integration scheme in the FDTD method for electromagnetic analysis, the discretized Maxwell's equations can be solved by an implicit numerical method on SPICE-like simulator [34]. Therefore, the work in [34] provides the models categorized into the lowest level in the top-down design and bottom-up verification methodologies. Fig. 6 shows the transient waveforms obtained via the proposed procedure and the model in [34], where both results are obtained by *Cadence Spectre*. Table 1 shows the CPU time comparisons. We can see from this table that the proposed procedure is much more efficient than the results [34]. This means that the proposed procedure provides a higher model to estimate lower effects.

Example 3: Interconnect with nonlinear termination on PCB

The simple PCB model shown in Fig. 7(a) was also analyzed by the FDTD method, where the cell size was 0.8 $[mm]$ in both x

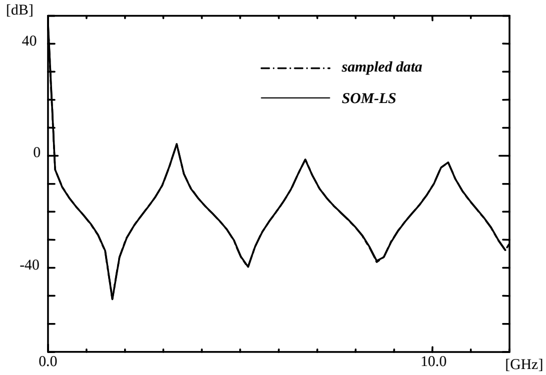

(a)

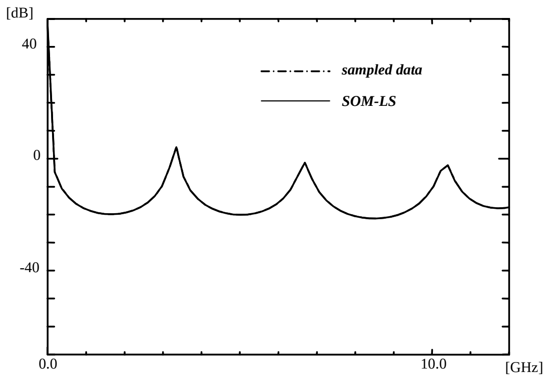

(b)

Figure 5: Approximation results of admittance parameters of the PCB model shown in Fig. 4. (a)$(1, 1)$ element. (b)$(2, 2)$ element.

Table 1: CPU time comparisons.

	ref.[20]	proposed
Example 2	550.94s	4.27s
Example 3	416.96s	4.09s

and y directions of the surface and 0.1 $[mm]$ in z direction. Then, the sampled data obtained by the FDTD method were represented by the rational matrix using the SOM-LS method. The SOM-LS method selected 8 poles from 306 poles.

The transient responses of the circuit with nonlinear termination shown in Fig. 7(b) were computed using *Cadence Spectre*. Fig. 8 shows the transient waveform which is compared with the work in [34]. As same with the previous example, we can see that the proposed procedure is very efficient.

4. Conclusions

The top-down design and bottom-up verification methodologies of mixed analog/digital circuits will be widely employed henceforth since it relaxes time-to-market pressures due to the continued consumerization of the electronics market place. Recently, it becomes indispensable to evaluate physical effects on interconnects and package which are obtained by sampled data via electromagnetic analysis or measurement in many cases. Therefore, describing multiport networks characterized by sampled data in an environment of the methodologies becomes very important. Hence, we presented the selective orthogonal matrix least-squares (SOM-LS) method for representing the sampled data with the rational matrix. This method allows us to construct the compact models since the sampled data are approximated, selected the dominant poles of the rational matrix.

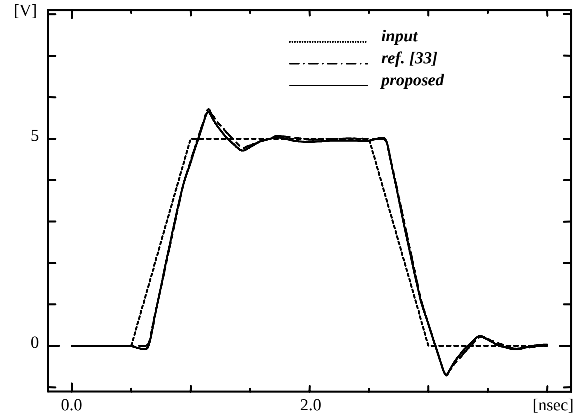

Figure 6: Transient voltage waveforms of V_2 shown in Fig. 4(b).

In the numerical examples, simple PCB models were described in the format of Verilog-A and the transient simulations were carried out on a commercial circuit simulator. We confirmed that the proposed procedure was very efficient.

The SOM-LS method generalizes the Chen's method [31] which is for SISO nonlinear system identification. Therefore, this method will be also applicable to modeling of MIMO nonlinear systems.

5. References

[1] Standard Description Language Based on the VerilogTM Hardware Description Language, IEEE Standard 1364, 1995.

[2] E. Christen and K. Bakalar, "VHDL-AMS -A hardware description language for analog and mixed-signal applications," *IEEE Trans. CAS-II*, vol. 46, no. 10, pp. 1263-1272, Oct. 1999.

[3] K. Kundert, H. Chang, D. Jefferies, G. Lamant, E. Malavasi, and F. Sendig, "Design of mixed-signal systems-on-a-chip," *IEEE Trans. CAD*, vol. 19, no. 12, pp. 1561-1571, Dec. 2000.

[4] T. Mukherjee, G. K. Fedder, D. Ramaswamy, J. White, "Emerging simulation approaches for micromachined devices," *IEEE Trans. CAD*, vol. 19, no. 12, pp. 1572-1589, Dec. 2000.

[5] B. D. Smedt and G. Gielen, "Model for Systematic Design and Verification of Frequency Synthesizer," *IEEE Trans. CAS-II*, vol. 46, no. 10, pp. 1301-1308, Oct. 1999.

[6] L. T. Pillage and R. A. Rohrer, "Asymptotic waveform evaluation for timing analysis," *IEEE Trans. Computer-Aided Design*, vol. 9, no. 4, pp. 352-366, Apr. 1990.

[7] E. Chiprout and M. S. Nakhla, "Analysis of interconnect networks using complex frequency hopping (CFH)," *IEEE Trans. Computer-Aided Design*, vol. 14, no. 2, pp. 186-220, Feb. 1995.

[8] P. Feldmann and R. W. Freund, "Efficient linear analysis by Padé approximation via the Lanczos process," *IEEE Trans. Computer-Aided Design*, vol. 14, no. 5, pp. 639-649, May 1995.

[9] L. M. Silveira, M. Kamon, I. Elfadel, and J. White, "A coordinate-transformed Arnoldi algorithm for generating guaranteed stable reduced-order models of RLC circuits," *in Proc. ICCAD'96*, pp. 288-294, 1996.

[10] K. J. Kerns and A. T. Yang, "Stable and efficient reduction of large, multiport RC networks by pole analysis via congruence transformations," *IEEE Trans. Computer-Aided Design*, vol. 16, no. 7, pp. 734-744, July 1997.

[11] A. Odabasioglu, M. Celik, and L. T. Pilleggi, "PRIMA: passive reduced-order interconnect macromodeling algorithm," *IEEE*

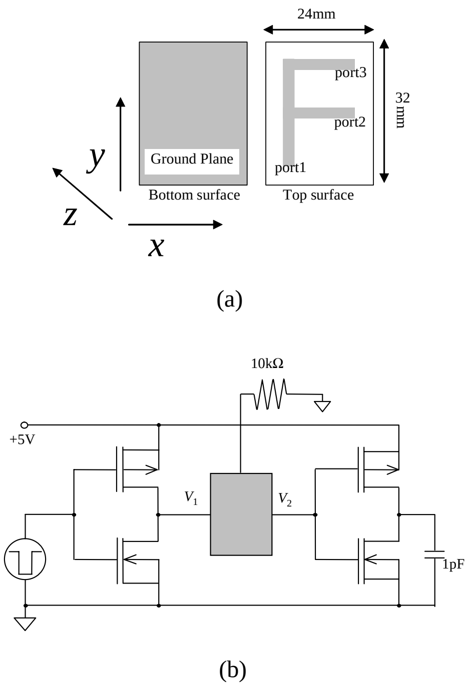

Figure 7: PCB model and circuit of *Example 3*. (a)PCB model. (b)Circuit.

Trans. Computer-Aided Design, vol. 17, no. 8, pp. 645-654, Aug. 1998.

[12] Z. Bai, R. D. Slone, W. T. Smith, and Q. Ye, "Error bound for reduced system model by Padé approximation via the Lanczos Process," *IEEE Trans. Computer-Aided Design*, vol. 18, no. 2, pp. 133-141, Feb. 1999.

[13] J. Roychowdhury, "Reduce-order modeling of time-varying systems," *IEEE Trans. CAS-II*, vol. 46, no. 10, pp. 1273-1288, Oct. 1999.

[14] M. Rewieéski and J. White, "A trajectory piecewise-linear approach to model order reduction and fast simulation of nonlinear circuits and micromachined devices," *IEEE Trans. Computer-Aided Design*, vol. 22, no. 2, pp. 155-170, Feb. 2003.

[15] J. R. Phillips, "Projection-based approaches for model reduction of weakly nonlinear, time-varying systems," *IEEE Trans. Computer-Aided Design*, vol. 22, no. 2, pp. 171- 187, Feb. 2003.

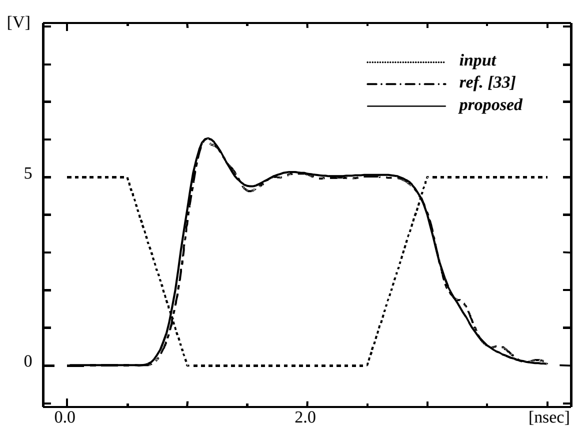

Figure 8: Transient voltage waveforms of V_2 shown in Fig. 7(b).

[16] P. P. Sylvester, "*Finite Elements for Wave Electromagnetics: Methods and Techniques*", IEEE Press, New York, 1994.

[17] R. F. Harrington, "*Field Computation by Moment Methods*", IEEE Press , New York, 1993.

[18] A. Taflove, "*Computational Electrodynamics: The Finite Difference Time Domain Method*", Artech House, Norwood, MA, 1995.

[19] L. M. Silveira, I. M. Elfadel, J. K. White, M. Chilukuri, and K. S. Kundert, "Efficient frequency-domain modeling and circuit simulation of transmission lines," *IEEE Trans. Comp., Packag., Manufact., Technol.-Part B*, vol. 17, no. 4, pp. 505-513, Nov. 1994.

[20] W. T. Beyene and J. E. Schutt-Aine, "Efficient transient simulation of high-speed interconnects characterized by sampled data," *IEEE Trans. Comp., Packag., Manufact., Technol.-Part B*, vol. 21, no. 1, pp. 105-114, Feb. 1998.

[21] M. Celik and A. C. Cangellaris, "Efficient transient simulation of lossy packaging interconnects using moment-matching techniques," *IEEE Trans. Comp., Packag., Manufact., Technol.-Part B*, vol. 19, pp. 64-73, Feb. 1996.

[22] K. L. Choi, N. Na, and M. Swaminathan, "Characterization of embedded passives using macromodels in LTTC technology," *IEEE Trans. Comp., Packag., Manufact., Technol.-Part B*, vol. 21, no. 3, pp. 258-268, Aug. 1998.

[23] T. Watanabe and H. Asai, "Synthesis of time-domain models for interconnects having 3-d structure based on FDTD Method", *IEEE Trans. Circuits and Syst.-II*, vol.47, no.4, pp.302-305, April 2000.

[24] Y. Tanji and M. Tanaka, "Hierarchical least-squares algorithm for macromodeling high-speed interconnects characterized by sampled Data," *IEICE Trans. on Fundamentals*, vol. E83-A, no. 9, pp. 1833-1843, Sep. 2000.

[25] M. Suzuki, H. Miyashita, A. Kamo, T. Watanabe and H. Asai, "A synthesis of time-domain interconnect models by mimo type of selective orthogonal least-square method", *IEEE Trans. Microwave Theory and Techniques*, vol. 49, no.10, pp.1708-1714, Oct. 2001.

[26] T. Mangold and P. Russer, "Full-wave modeling and automatic equivalent-circuit generation of millimeter-wave planar and multi-layer structures," *IEEE Trans. Microwave and Theory Tech.*, vol. 47, no. 6, pp. 851-858, June 1999.

[27] D. Saraswat, R. Achar, and M. Nakhla, "A fast algorithm and practical considerations for passive macromodeling of measured/simulated data," *in Proc. 11th Topical Meeting Electrical Performance Electron. Packag.*, pp. 297-300, 2002.

[28] I. S. Stievano, D. Becker, F. G. Canavero, Z. Chen, G. Katopis, I. A. Maio, "Behavioral modeling of IC ports including temperature effects," *in Proc. 11th Topical Meeting Electrical Performace Electron. Packag.*, pp. 333-336, 2002.

[29] A. I. Mees, M. F. Jackson, and L. O. Chua, "Devices modeling by radial basis functions," *IEEE Trans. CAS-I*, vol. 39, no. 1, pp. 19-27, 1992.

[30] S. Chen, C. F. N. Cowan, and P. M. Grant, "Orthogonal least squares learning algorithm for radial basis function networks," *IEEE Trans. Neural Networks*, vol. 2, no. 2, pp. 302-309, 1991.

[31] S. Chen, S. A. Billings, and W. Luo, "Orthogonal least squares methods and their application to non-linear system identification," *Int. J. Control*, vol. 50, pp. 1973-1896, 1989.

[32] R. Achar, P. K. Gunupudi, and M. Nakhla, and E. Chiprout, "Passive Interconnect Reduction Algorithm for Distributed/Measured Networks," *IEEE Trans. CAS-II*, vol. 47, no. 4, pp. 287-301, 2000.

[33] G. H. Golub and C. F. V. Loan, "Matrix Computations," The Johns Hopkins University Press, 1996.

[34] W. Sui, A. Christensen, C. H. Durney, "Extending the two-dimensional fdtd method to hybrid electromagnetic systems with active and passive lumped elements," *IEEE Trans. MTT*, vol. 40, no. 4, pp. 724-730, Apr. 1992.

[35] *Affirmaa Spectrea Circuit Simulator User Guide*.